Research Article

Gelatin Used as a Transductor in an Optical Hygrometer Based on a Fabry-Perot Interferometer

Sergio Calixto [ID]

Centro De Investigaciones En Optica, Loma Del Bosque 115, Leon, Gto C.P. 37150, Mexico

Correspondence should be addressed to Sergio Calixto; scalixto@cio.mx

The quantities that are usually measured are time, pressure, temperature, and relative humidity to mention but a few. The word humidity is used when we are dealing with water vapor which is a gas. The instrument used to measure the humidity is the hygrometer that can be based on electronics, optics, mechanics, chemicals, and others. The measurement of humidity shows its importance in applications such as food processing, meteorological, semiconductor, building and construction, medical, and automotive to mention but a few. This paper shows the adaptation of an optical interferometer, the Fabry-Perot (*F-P*), to measure the relative humidity. The transductors that have been probed are gelatin-thin films that are inserted between the mirrors of the FP. When water molecules are absorbed (desorbed) by the gelatin film, its refractive index and thickness change giving a movement of the rings in the interference pattern. The calibration plot comprises the ring displacement as a function of the relative humidity.

1. Introduction

It is understood that the term humidity refers to the presence of water in gaseous form. Relative humidity is defined [1] as the ratio of the amount of water vapor present in the atmosphere to the maximum amount the atmosphere can hold and is expressed as a percentage.

To monitor humidity, several techniques have been employed. There are different sensors based on electronics [2] (miniaturized electronic sensors), mass change (based on the principle of resonant frequency), mechanical (using synthetic fibers and human hair), and optical (like chilled mirror hygrometer), for example. Electronic sensors [2] can be classified by the transduction scheme that they use to convert water vapor concentration into an electrical signal: capacitive [3, 4], resistive (DC resistance or AC impedance) [3, 4], and advanced resistive (piezoresistive). Each sensor has advantages and disadvantages yet none of them can fulfil the majority of the requirements; thus, each one is used in a different case. The key component in the RH sensors is the transductor that interacts with the water molecules. The ideal sensing film material will have characteristics such as high sensitivity to water molecules, linear response from 0% to 100% RH, short response time, and long-term stability to mention but a few.

The optical RH sensors are the ones based on optical fibers [5] and on holographic devices [6–8], for example. The fiber optics sensors use the techniques such as direct spectroscopic, evanescent wave, in-fiber grating, and interferometric methods. Regarding the holographic sensors, there is one that uses a reflection hologram for visual indication of environmental humidity. The material that is used to fabricate the hologram is a photopolymer. Once the hologram is made, white light is sent to it and the reflected light is analyzed. If the atmosphere humidity surrounding the hologram changes, the reflected light will change color. When the humidity returns to the original first value, the color reflected by the hologram will return to his original value. That means it is reversible. The range of color change, reversibility, and the response time of the hologram have been studied in a controlled humidity environment. Holograms with response times from few seconds to tens of minutes have been designed. Another sensor based on color changes is mentioned in reference [9].

An optical structure that is based on multiple reflections and shows high sensitivity is the Fabry-Perot interferometer (*F-P*) [10]. When the F-P was developed about 100 years ago, it consisted of two mirrors, each one of them had a high reflectance thin film. However, the *F-P* now has suffered modifications when it is used in the photonics field. Some photonic devices use two fiber Bragg gratings (FBG) instead of mirrors as high reflectance mediums. Between the FBGs, an erbium-doped fiber (EDF) can be inserted forming a nonlinear FP. In references [11, 12], the optical bistability of this EBD-FP device has been studied under different parameters. Switching powers of about 7 mW have been found. In other work [13], Bragg gratings (BGs) have been incorporated in polymer photonic crystal waveguides (PPCWs) which have been generated by femtosecond lasers. The structure of the waveguide is inspired by the solid core photonic crystal fibers. PPCWs were fabricated with a depth of 300 microns below the surface of a transparent PMMA block. BGs were integrated into the core of PPCWs.

Also, another structure containing a *F-P* interferometer can be made with the use of two distributed Bragg reflectors (DBRs) whose center wavelength is controlled by insertion between the DBRs of a transmissive metasurface layer which behaves as a phase-shifting element enabling independent control of the filter passbands [14, 15]. Different geometries of the metasurfaces can be inserted in the cavity changing the resonant wavelength. DBR could be made of 4 pairs of α-SiO$_2$ quarter wave stacks.

Other application of *F-P* cavities is made in the fabrication of photonic-atom lasers with high spectral purity [16]. The laser 2.5 cm long is integrated into a micromachined rubidium vapor cell. It has a 20000 finesse and an ultra-narrow-line width of 25 Hz.

Here, we propose the interferometer *F-P*, based on multiple reflections, to monitor RH [10]. The interferometer comprises two high reflectance mirrors separated by a spacing. At the output of the interferometer, there is an interference pattern that consists of rings. The width of the rings is a function of the reflectance of the mirrors, and when the reflectance is high, the width is very narrow. The diameter of rings is a function of the spacing between the mirrors, the shorter the spacing, the longer the diameter. Another parameter that affects the rings is the refractive index of the medium that is between the mirrors. When the medium changes, the diameter of the rings is modified. Thus, we have inserted a hydrophilic material between the mirrors that change its thickness and refractive index, that is, its optical path, when the relative humidity increases or decreases. The rings will change their diameter accordingly to the humidity.

In Section 2 some hydrophilic materials are mentioned; among them, the gelatin that is the material has been chosen to insert between the mirrors. In Section 3, the *F-P* interferometer from the theoretical point of view is described. In Section 4, the experimental process to fabricate the gelatin thin films, the description of a homemade climatic chamber, and the results of the experiments are shown. A discussion about the versatility of the method comprising the *F-P* and the gelatin is presented in Section 5. Finally, we close with the conclusions.

2. Relative Humidity Sensor Materials

Among the materials used, transductors in optical RH sensors are [5] perylene and rhodamine dyes, agarose, PVA, polyimide, PTFE, phenol, PVDF, acrylamide, aluminosilicate, fluorophore in hydrogel films, interpenetrated polymers [17, 18], and many others. Here, we suggest the use of gelatin.

Gelatin is colorless, odorless, tasteless, nonsoluble in organic solvents, environmentally friendly, easy to handle and to purchase, and cost-effective, and in addition, it displays good clarity, biocompatibility, and biodegradability, among other characteristics. Moreover, the properties of gelatin such as its viscosity, gel strength, softening behavior, thixotropy, and melting point can be modified by UV light, heat, chemicals, and ultrasound. Chemical reactions introduce permanent cross-links between gelatin chains, a process called hardening. Aluminum and chromium are chemical hardeners. UV light involves a temporary rupture of certain bonds, resulting in a rearrangement of a more stable structure.

Gelatin [19, 20] is a natural product made by the hydrolysis of collagen. The source of collagen is normally either hide or bone that has been extracted with acid to remove minerals. The hydrolysis may be conducted either in a basic solution or acid. The purity of gelatin depends on the source of collagen and its treatment prior to hydrolysis. Gelatin is a protein, and its large molecules are synthesized in nature from many molecules of amino acids.

Air-dried gelatin [21] contains 8 to 15 percent of moisture, depending on the conditions under which it is dried. As for dried gelatin in contact with water vapor, the absorbed water molecules are a function of the relative humidity of the environment and of some other factors. The moisture taken up at a fixed RH depends on the pH of the original solution before gelation and drying. It is generally believed that the polar side chains of amino acid residues such as tyrosine, lysine, arginine, and glutamic acid provide much of the attraction for water molecules, and thus, the number and availability of the polar groups determine the amount of water a protein is able to absorb. The moisture is held by different forces depending on the RH value. Between the region 0% and 6% RH, water molecules are held to polar groups by hydrogen bonding. One water molecule is first bound tightly to two cooperating polar groups. Then, a second water molecule is added, giving a total of one water molecule per polar group. Additional water molecules attach themselves, and as RH increases, the absorption continues, and a complete layer of water is sandwiched into each space between protein layers. It has been shown that local sites for absorption are not limited to the surface layer of the protein, but they can be distributed through the lattice, exhibiting changes in cellular dimensions. When the RH surpasses 70%, the new absorved water molecules attach or condense to the old water molecules previously attached to the amino groups. This phenomena happens quickly [21–23]. At 95% RH, six or seven water layers are introduced between each layer and each neighboring layer. All the water molecules absorbed in this step are held by hydrogen bonds. The
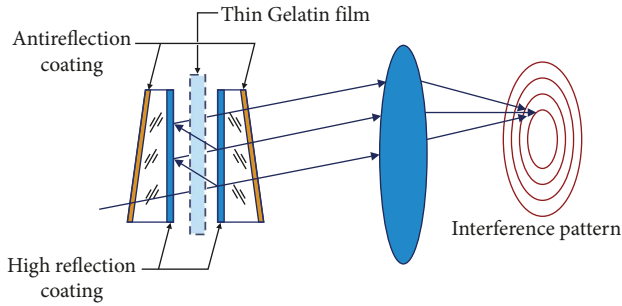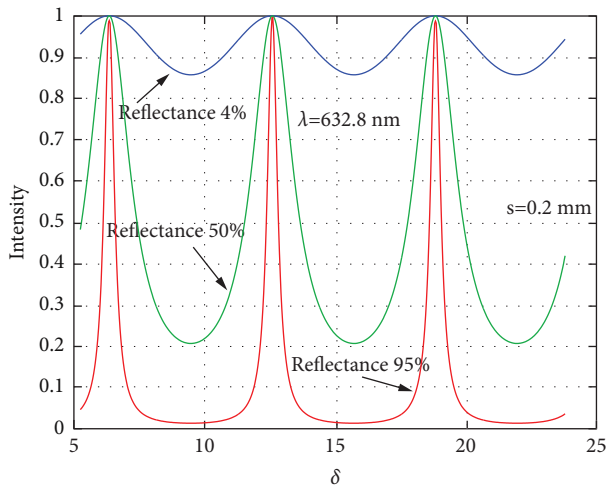
FIGURE 1: Scheme of a *F-P* interferometer.

FIGURE 2: Transmitted intensity as a function of δ for a *F-P* interferometer where a wavelength of 632.8 nm has been considered. The parameter is the mirrors' reflectance.

FIGURE 3: Transmitted intensity of a line of the interference pattern as a function of δ for a *F-P* interferometer. The parameter is the spacing s between the mirrors. The interference line has a movement in the right direction when the spacing decreases.

absorption of water at high relative humidity depends, however, on the prior sorption on active sorptive groups.

When water vapor is absorbed by (desorbed from) the gelatin films, its thickness changes. From the optical point of view, the absorption (desorption) of water vapor by the gelatin films will also affect its refractive index. When gelatin is dried, its refractive index is about 1.5. But when water is absorbed by the gelatin, we expect that the refractive index of gelatin diminishes because the water refractive index is 1.33. Regarding its thickness, it will be minimum when the film is dry and maximum when the film is swollen [24, 25]. These changes in refractive index and thickness due to absorption (desorption) of environmental water vapor can be monitored with a two wave interferometer, the Mach-Zehnder [17–26].

3. Fabry-Perot Interferometer (Theory)

The basic configuration of a *F-P* interferometer [10] is shown in Figure 1. Two mirrors with flat surfaces form the cavity. Each mirror has two surfaces, one that is called the inner surface, that is inside the cavity, and the other called the outer surface. The inner surface has a thin film that could be made of aluminium or a multilayer thin film stack. On the outer faces of the mirrors, there is an antirefl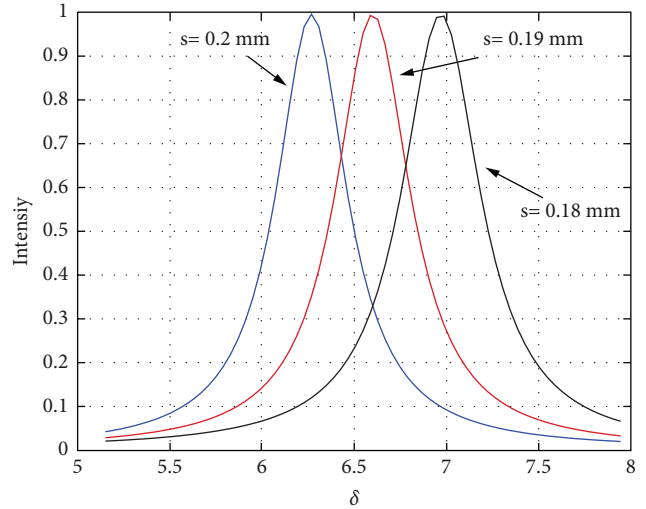ection coating. This last face is at a small angle to avoid the interference pattern given by the reflections coming from this outer surface.

The equation that describes the Fabry-Perot transmitted intensity is [10]

$$I_T = \frac{I_0}{\left(1 + \left(4R^2 / \left(1 - R^2\right)\right)\right)} \sin^2 \left(\frac{\delta}{2}\right), \qquad (1)$$

where the phase $\delta = (4\pi/\lambda)$ ns cos φ. Here, s is the spacing between the inner faces of the mirrors, n is the refractive index of the material between the mirrors, R^2 is the reflectance, and λ is the wavelength (632.8 nm). Figure 2 shows the transmitted intensity as a function δ. In the graph, a spacing between the mirrors of 0.2 mm has been considered along with the following values of reflectances: 0.04, 0.50, and 0.95.

It is noted that the curve when reflectance has a value of 4% looks like a $\cos^2$ contour obtained from the interference of two beams. It is not exactly the same, however, and the resemblance holds only when the reflectance is small. Then, the first two reflected beams are so much stronger than the rest that have little effect [10, 13]. As the reflectance of the surfaces is increased, the fringes due to multiple reflections become narrower.

It is possible to consider theoretically the position of an interference line of the pattern when several spacings *s* between the mirrors are taken as a parameter. This spacing is included in the phase of equation (1). The next graphs, Figure 3, show the intensity of a light line of the interference pattern as a function of the delta phase when several spacings *s* between the mirrors are considered. When the spacing decreases, a movement of the line in the right direction can be seen. This phenomenon happens in the experiments described in Section 4.
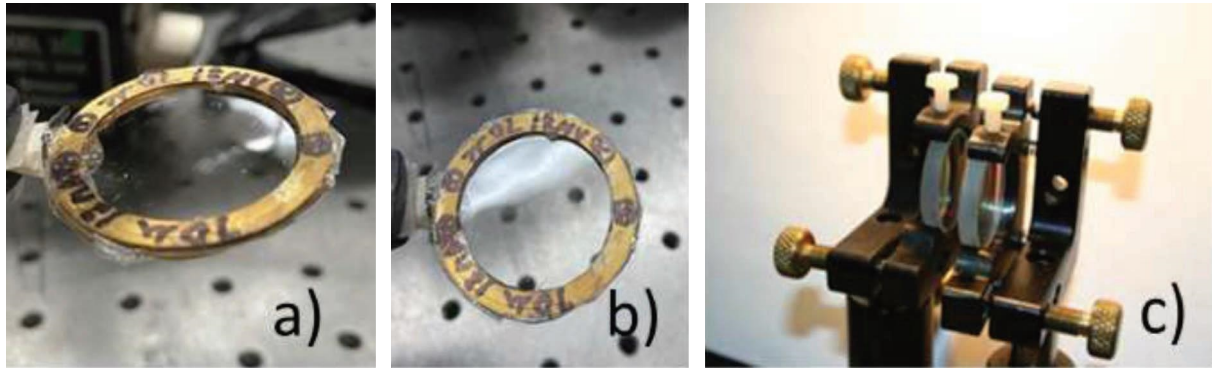
FIGURE 4: (a), (b) Metallic O-ring with a diameter of about 4 cm and thickness of 1 mm. A thin gelatin film was glued to the ring. (c) Fabry-Perot with two high reflecting mirrors.
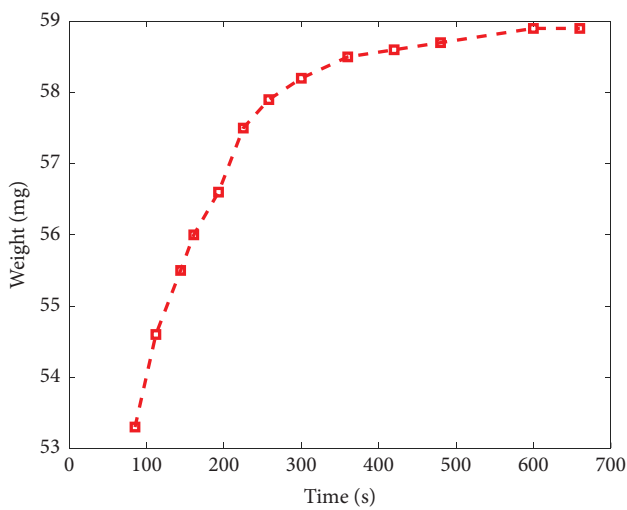

FIGURE 5: Behavior of gelatin weight as a function of time when the gelatin film absorbed water molecules from an atmosphere with a 46% RH.

FIGURE 6: Reflectance of F-P mirrors as a function of wavelength.

4. Fabry-Perot Interferometer as Relative Humidity Sensor (Experimental)

The gelatin thin films behaved like a humidity sensor when fabricated with the following method [27]. A solution of 2% gelatin with distilled water was prepared. Then, the part of it was poured onto a leveled flat glass surface. The poured amount depended on the desired thickness. After some hours, the solution dried, and a thin film of gelatin was present. Gelatin films with thickness from about 10 microns till 70 microns were fabricated. After the drying period, a metallic ring of about 34 mm diameter with a thickness of 1 mm was glued to the gelatin film. Then, the ring and gelatin film were detached from the glass surface, Figure 4. The ring was placed between the mirrors of the F-P interferometer. The distance between them was about 3 mm. The interference pattern after the insertion of the ring showed a little distortion.

A gravimetric analysis of the gelatin film absorption of water molecules was done by measuring its weight when a constant RH was present [18]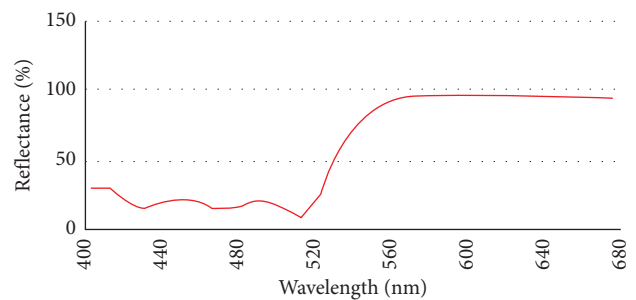. First, the film was placed in a box that contained silica gel for an hour. During this time, the film dried. Then, it was placed in the balance. Room RH and temperature were 46% and 24°C, respectively. The film began absorbing water molecules and swell with the result that its weight increased with time. Figure 5 shows the weight change behavior as a function of time. At first, it increases, and then, it stabilizes. From this plot, we can say that it attains about the 98% of its weight (58 mg) in about 220 s that would be its response time.

Dry gelatin absorbs water from a humid atmosphere or from the liquid until it has absorbed a definite amount and has reached an equilibrium state, which is dependent on relative humidity and temperature. The moisture taken up at a fixed relative humidity depends upon the pH to which the original gel solution was adjusted before drying.

The mirrors of the F-P interferometer used in the experiments had a stack of thin films with a reflectance of 99%, Figure 6. With this value, the fringes presented a narrow profile. A He-Ne laser ($\lambda = 632.8$ nm) was used as the light source.

The method to control the RH was implemented in the laboratory by fabricating a climatic chamber that consisted of a plastic box where the F-P interferometer was placed together with an electronic hygrometer [28] used for calibration. The plastic box had a hose connection with an air pump which in turn was connected to a cylinder filled with silica gel. This cylinder had a hose connection with the box. The pump extracted the water molecules from the box and then inserted dry air so RH was diminished. Inside the box, a petri dish that contained water was placed. The dish had a

glass cover that could be slided. When an increment of RH was needed the cover was slided. The lid of the petri dish was opened after the injection of dry air. Water molecules began to fill the box and were absorbed by the gelatin film that changed its refractive index and thickness which resulted in a movement of the interference pattern lines. This pattern was overlapped on a reticle that had a linear scale. The movement of an interference line relative to the linear scale was monitored with a microscope.

In Section 3, it has been mentioned that the interference pattern given by the *F-P* interferometer shows fringes that become very narrow for high values of the reflectivity, and then, the position of each fringe can be measured with high precision. Besides, it has been mentioned in Section 2 that when gelatin absorbs water molecules, its refractive index diminishes, and its thickness increases. These parameters are included in the phase of the equation mentioned in Section 3.1. Thus, it is seen that the position of the fringes will change when water molecules are absorbed (desorbed) by a gelatin thin film that is placed between the mirrors of the *F-P* interferometer. Photograph in Figure 7 shows some interference fringes given by the *F-P*. It is noticed that the fringes are narrow. A note here regarding the width of the fringes in the photograph is given now. Exposure time to take the photograph was long because with this method, the reticle image became clearer. This long exposure increased the interference lines' thickness. During the measurements, the fringes' width seen with the eye was narrower.

Figure 8 shows the behavior of a normalized interference line displacement as a function of the RH. The parameter is the gelatin film thickness. It is noted that for the measurements, the first interference line that is closer to the center of the interference pattern was chosen. From the plot, we can see that as the RH increases, also the distance traveled by the interference line increases. Different film thicknesses were used. As the thickness of the gelatin film increases, its slope is more pronounced because it absorbs more water molecules, and its thickness increases more than the thinner films. The slope of these plots is the sensitivity.

Linear interpolation of the experimental points shown in Figure 8 was done with the Excell program. In the calculations, the original values given by the experiment were used and not the normalized ones presented in Figure 8. The results for each plot, that is, for each gelatin film thickness, are shown in Figure 9. There, it is possible to see the equations of the interpolated points. The slopes or sensitivity for the different gelatin films thickness are as follows: for $70\,\mu$m thickness, 0.0447 mm/RH%; for $50\,\mu$m thickness, 0.0339 mm/RH%; and for $20\,\mu$m thickness, 0.0323 mm/RH%. Thus, a better sensitivity is shown by thick films.

A note is given about the use of gelatin-thin films. As can be seen in Figure 9, the plots span from about 20% RH till about 45%. At low RH values, the gelatin surface is tense, but when RH values higher than 45% are present, the film presents a loose surface, and the interference pattern gets blurred. The interference line position on the reticle is
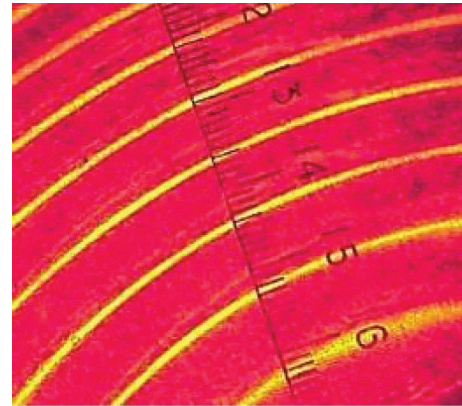

FIGURE 7: Photograph showing some interference fringes given by a *F-P* interferometer. A reticle was overlapped with the fringes. Minimum distance in the reticle was 0.1 mm.
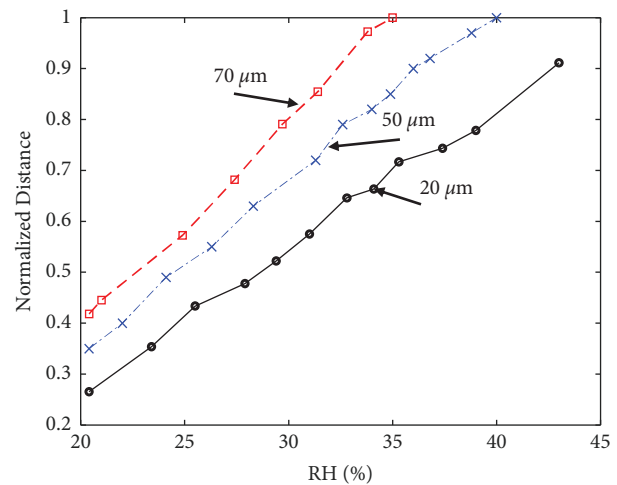

FIGURE 8: Normalized interference line displacement as a function of relative humidity (%). The parameter is the gelatin film thickness.

difficult to assess. However, this difficulty can be overpassed when thicker films are used. Thus, we can choose the RH range where the interferometer can be used.

Regarding the hysteresis, an experiment was done where RH was increased by opening the lid of the petri dish. RH increased until a maximum, and then, the lid of the dish was closed, and the RH decreased. Result can be seen in Figure 10. It seems that it is more difficult for the gelatin film to lose water molecules.

5. Discussion

Throughout the paper, it has been shown the use of a *F-P* interferometer as a hygrometer. The method shows versatility because the transductor, i.e., the gelatin, and the optical instrument, the *F-P*, can be adapted to the experimental needs. This includes the sensitivity.
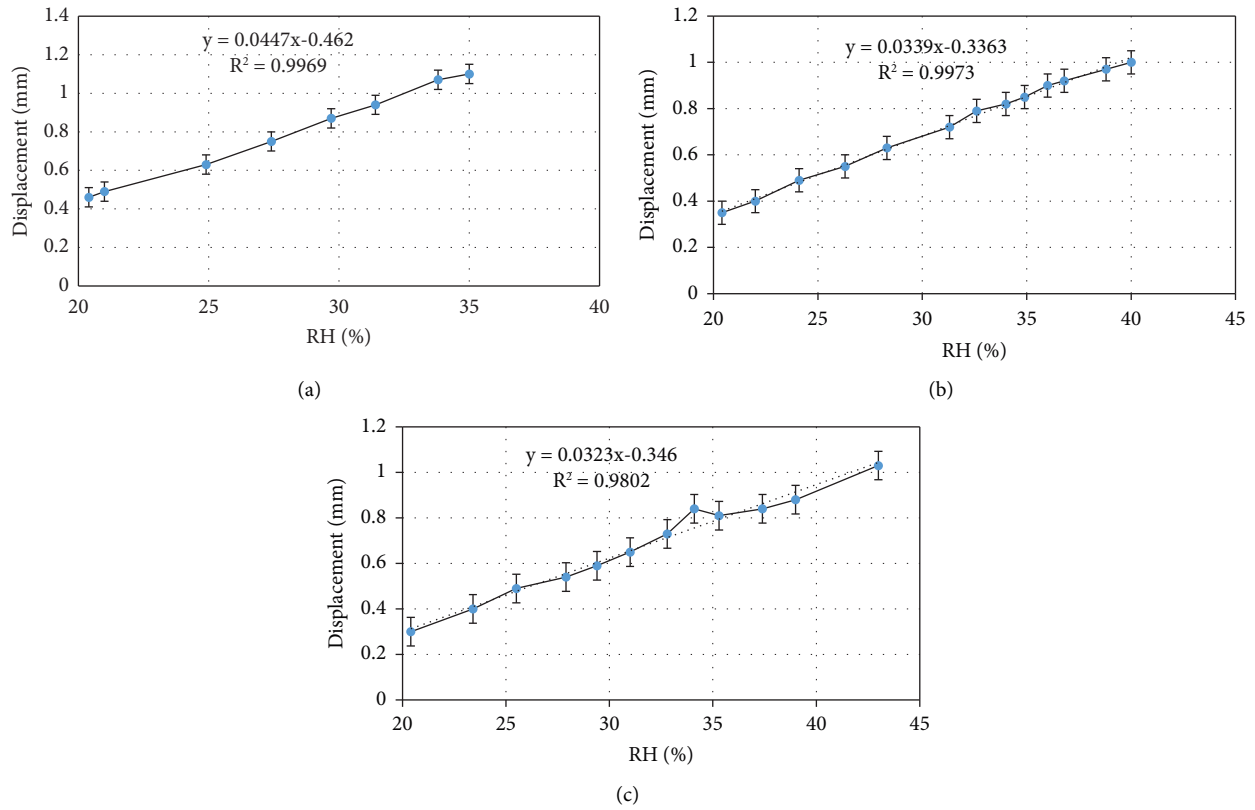
(a)

(b)

(c)

FIGURE 9: Interference line displacement as a function of RH (%). Film thickness in (a) 70 μm, (b) 50 μm, and (c) 20 μm. Vertical error bars are 0.1 mm. There are no horizontal error bars because the electronic hygrometer had the reading till the first digit after the point or tenths of relative humidity integers.
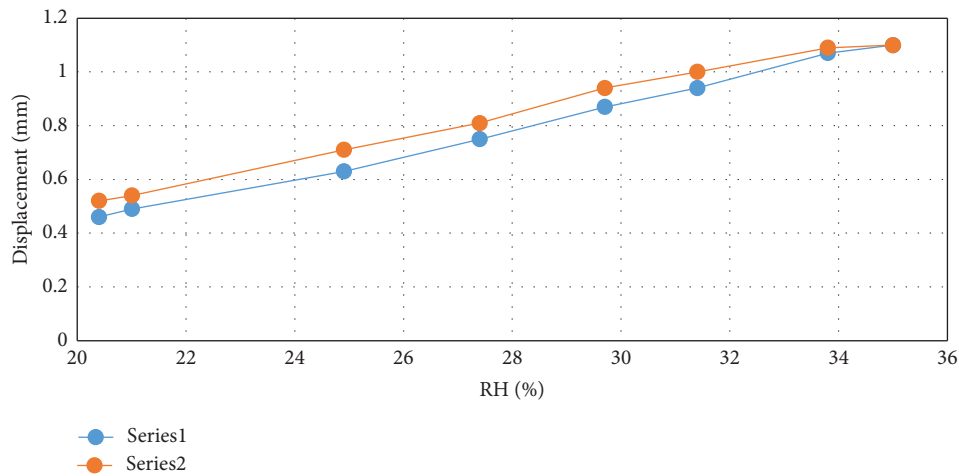

FIGURE 10: Plots show the behavior of the interference line displacement as a function of RH%. Series 1 (blue color) shows when the RH was rising and series 2 (red color) when RH decreased.

Regarding the transductor from the very beginning of its fabrication, it can be tailored to the needs by selecting the method and the materials to fabricate the gelatin powder. For example, the gelatin swelling, which includes the change of refractive index and the thickness of the films, can be modified by selecting the pH of the mixture in the fabrication step [29]. There are roughly three classes of photographic gelatins: hard, medium, and soft-which can be differentiated by their setting and melting points, and by the quantity of water, they will absorb. The viscosity of most gelatins can be very largely controlled in an emulsion by the modification of the concentration, by the addition of alcohol or acetone, or by the addition of chrome alum, formalin, or sodium sulfate. However, if the gelatin is acquired from a company, its approximate viscosity and hardness can be mentioned to the gelatin manufacturers. Once it is

TABLE 1: Characteristics of some hygrometers.

	HC2A-S	MEMS SENSOR	Chipcap2
Operating range	0–100%	50%–90%	0–100%
Accuracy	±0.8%	Sensitivity 0.065 Pf/RH%	±3%
Manufacturer	PST processing sensing technologies [30]	[31]	Amphenol [32]. Based on MEMS technology.

fabricated, its properties such as its viscosity, gel strength, softening behavior, thixotropy, and melting point can be modified by UV light, heat, chemicals, and ultrasound. Regarding the RH range where the method has been proved that goes from 20% to 45%, it can be extended by the use of thicker films. In this way, the film will not show a loose surface.

The *F-P* also can be adapted to the experimental needs. The width of the interference lines can be controlled by the reflectivity of the mirrors. A small width means more precision can be attained. To control and increase the precision of the measurements, the parameters of the reticle can be selected. Regarding the interference lines displacement, it can be amplified by using long focal distance lenses. This will increase the diameter of the ring pattern and will give more precision.

Gelatin thin films can be adapted to control its sensitivity by changing its porosity [3]. There are methods that can be used to increase the porosity, and thus, the water molecules will penetrate (absorbed or desorbed) more easily. However, it should be considered that more porosity will mean more scattering that will affect the definition of the interference lines.

It was mentioned at the Introduction that sensors have advantages and disadvantages but none of them can fulfill the majority of the requirements. For example, Table 1 exposed the characteristics of some electronic RH sensors. It is possible to see that they perform better that the F-P interferometer sensor described in this paper. But unfortunately, they use electricity which can be dangerous when explosive environments or materials are present.

The *F-P* interferometer that was built had mirrors with a diameter of about 2.5 cm, lens with a diameter of 3 cm, and focal length of 10 cm. Here, it is suggested a means to miniaturize the configuration. The *F-P* structure could be made smaller by using mirrors and lens with a diameter of say 8 mm. Instead of having a reticle, the position of a fringe could be read with a linear CCD. The material used to separate the mirrors should be temperature-independent. A structure to fix the gelatin thin film between the mirrors should be present. An aperture between the mirrors should be included to let air pass.

The possibility to use the gelatin as a long-term transductor depends mainly on the biodeterioration caused by fungi (lichenized fungi or lichens), bacteria, and microalgae [33, 34]. Fungi can tolerate lower humidity and a wide range of temperatures than the other two and can be easily transported by air. Gelatin is affected by *P. chrysogenum, A. versicolor, P. glomerata, M. rocemasus, Alternaria alternata, Aspergillus ustus, Trichoderma, C. cladosporioides, Aspergillus nidulans,* and penicillium to produce mineralization or cause variable biodeterioration rates, from 5% to 30%.

6. Conclusions

Each hygrometer sensor has advantages and disadvantages yet none of them can fulfil the majority of the requirements; thus, each one is used in a different instance. Here, we have shown that the *F-P* interferometer, together with gelatin-thin films as transductors, can be used as a hygrometer. Calibration plots considering different gelatin films have been shown.

Data Availability

No data were used to support this study.

Conflicts of Interest

The authors declare no conflicts of interest.

Acknowledgments

References

[1] P. Wiederhold, *Water Vapor Measurements Methods and Instrumentation*, Marcel Dekker, New York NY, USA, 1997.

[2] R. Fenner and E. Zdankiewicz, "Micromachined water vapor sensors: a review of sensing technologies," *IEEE Sensors Journal*, vol. 1, no. 4, pp. 309–317, 2001.

[3] C. Doroftei and L. Leontie, "Porous nanostructured gadolinium aluminate for high-sensitivity humidity sensors," *Materials*, vol. 14, no. 22, p. 7102, 2021.

[4] Y. Zhang, B. Li, and Y. Jia, "High humidity response of sol–gel-synthesized BiFeO3 ferroelectric film," *Materials*, vol. 15, no. 8, p. 2932, 2022.

[5] T. L. Yeo, T. Sun, and K. T. V. Grattan, "Fibre-optic sensor technologies for humidity and moisture measurement," *Sensors and Actuators A: Physical*, vol. 144, no. 2, pp. 280–295, 2008.

[6] I. Naydenova, R. Jallapuram, V. toal, and S. Martin, "A visual indication of environmental humidity using a color changing hologram recorded in a self-developing photopolymer," *Applied Physics Letters*, vol. 92, no. 3, p. 031109, 2008.

[7] I. Naydenova, R. Jallupuran, V. Toal, and S Martin, "Characterization of the humidity and temperature responses of a reflection hologram recorded in acrylamide –based photoplymer," *Sens. Actuat. B – chem*, vol. 139, no. 1, pp. 35–38, 2009.

[8] T. Mikulchyk, S. Martin, and I. Naydenova, "Investigation of the sensitivity to humidity of an acrylamide-based photopolymer containing N-phenylglycine as a photoinitiator," *Optical Materials*, vol. 37, pp. 810–815, 2014.

[9] J. C. Tellis, C. A. Strulson, M. M. Myers, and K. A. Kneas, "Relative humidity sensors based on an environment-

sensitive fluorophore in hydrogel films," *Analytical Chemistry*, vol. 83, no. 3, pp. 928–932, 2011.

[10] F. A. Jenkins and H. E. White, *Fundamentals of Optics*, McGraw-Hill, New York, NY, USA, 1957.

[11] Z.-gang Zang and W.-xuan Yang, "Theoretical and experimental investigation of all-optical switching based on cascaded LPFGs separated by an erbium-doped fiber," *Journal of Applied Physics*, vol. 109, no. 10, p. 103106, 2011.

[12] Z. Zang, "Numerical analysis of optical bistability based on Fiber Bragg Grating cavity containing a high nonlinearity doped-fiber," *Optics Communications*, vol. 285, no. 5, pp. 521–526, 2012.

[13] G. Roth, S. Kefer, S. Hessler, C. Esen, and R. Hellmann, "Polymer photonic crystal waveguides generated by femtosecond laser," *Laser & Photonics Reviews*, vol. 15, no. 11, Article ID 2100215, 2021.

[14] Y. Horie, A. Arbabi, E. Arbabi, S. M. Kamali, and A. Faraon, "Wide bandwidth and high resolution planar filter array based on DBR-metasurface-DBR structures," *Optics Express*, vol. 24, no. 11, Article ID 11677, 2016.

[15] F. Ali and H. Mosallaei, "A tunable semiconductor-based transmissive metasurface: dynamic phase control with high transmission level," *Laser & Photonics Reviews*, vol. 14, 2020.

[16] W. Zhang, L. stern, D. Carlson et al., "Papp, ultranarrow linewidth photonic-atomic laser," *Laser & Photonics Reviews*, vol. 14, 2020.

[17] S. Calixto, M.-E. Calixto-Olalde, J. Hernandez-Barajas, and O. Vazquez-Espitia, "Mach-Zehnder interferometer applied to the study of polymer's Relative Humidity Response," in *Proceedings of the MOEMS and Miniaturized Systems*, San Francisco, CA, USA, February 2018.

[18] S. Calixto, V. Piazza, and V. Marañon-Ruiz, "Stimuli-Responsive systems in optical humidity-detection devices," *Materials*, vol. 12, no. 2, p. 327, 2019.

[19] GELITA, Uferstrabe, Eberbach, Germany, 2018, https://www.gelita.com.

[20] C. E. K. Mees, *The Theory of the Photographic Process*, McMillan, New York, NY USA, 1954.

[21] J. Kosar, *Light-Sensitive Systems: Chemistry and Application of Nonsilver Halide Photographic Processes*, John Wiley & Sons, Hoboken, NJ, USA, 1965.

[22] E. F. Mellon, A. H. Korn, and S. R. Hoover, "Water absorption of proteins. I. The effect of free amino groups in casein," *Journal of the American Chemical Society*, vol. 69, no. 4, pp. 827–831, 1947.

[23] A. B. D. Cassie, "Multimolecular absorption," *Transactions of the Faraday Society*, vol. 41, pp. 450–458, 1945.

[24] A. Green and G. I. P. Levenson, "A practical swellmeter," *Journal of Photographic Science*, vol. 20, no. 6, pp. 205–210, 1972.

[25] N. D. Levine and H. A. Levine, "Zoonoses," *Science*, vol. 143, no. 3613, pp. 1464–1466, 1964.

[26] S. Calixto, "Arely Montes-Perez, "An interferometric humidity sensor based on a thin gelatin film," in *Proceedings of the SPIE 9203, Interferometry XVII: Techniques and Analysis*, Article ID 920318, San Diego California, USA, August 2014.

[27] G Sigma-Aldrich, *Product Gelatin, Type B from Bovine Skin, Sigma-Aldrich*, Saint Louis, MO, USA.

[28] Extech Instruments Corporation, *Moisture Meter Model MO210*, Extech Instruments Corporation, Waltham, MA,USA.

[29] B. H. Carrol, G. C. Higgins, and T. H. James, *Introduction to Photographic Theory*, John Wiley & Sons, New York NY, USA, 1980.

[30] Processing Sensing, *Processing Sensing Technologies*, https://www.processingsensing.com/en-us/contact/, 2022.

[31] S. Shapardanis, M. Hudpeth, and T. Kaya, "Gelatin as a new humidity sensing material: characterization and limitations," *AIP Advances*, vol. 4, no. 12, pp. 127132–132, 2014.

[32] Newark.com, "Newark.com," *Catalog Page*, https://www.newark.com, 1884.

[33] J. Kosel and P. Ropret, "Overview of fungal isolates on heritage collections of photographic materials and their biological potency," *Journal of Cultural Heritage*, vol. 48, no. 2021, pp. 277–291, 2021.

[34] E. D. O. T. Bezerra and T. Bezerra, S. B. R. Berton, A de Oliveira, P. R. Souza et al., The cooling of blends in water supports durable, thermo-responsive, and porous gelatin-polyphenolic tannin assemblies with antimicrobial activities," *Materials Today Communications*, vol. 26, Article ID 101883, 2021.